

Simultaneous constraints on bias, normalization and growth index through power spectrum measurements

Cinzia Di Porto^{1,2}, Luca Amendola², Enzo Branchini³

¹*INAF-Osservatorio Astronomico di Bologna, Via Ranzani 1, 40127, Bologna, Italy and INFN Sezione di Bologna*

²*Institut für Theoretische Physik, Universität Heidelberg, Philosophenweg 16, 69120 Heidelberg, Germany*

³*Dipartimento di Fisica “E. Amaldi”, Università degli Studi “Roma Tre”, via della Vasca Navale 84, 00146, Roma, Italy, INFN Sezione di Roma Tre and INAF, Osservatorio Astronomico di Brera, Milano, Italy*

Submitted:

ABSTRACT

In this Letter we point out that redshift surveys can break the degeneracy between the galaxy bias, the power spectrum normalization, $\sigma_{8,0}$ and the growth factor, without the need for external information by using a simple and rather general parametrization for the growth rate, the well known γ parametrization and measuring the power spectrum at least at two different redshifts. We find that in next-generation surveys like Euclid, $\sigma_{8,0}$ and γ can be measured to within 1% and 5%, respectively, while the bias $b(z)$ can be measured to within 1 – 2% in each of 14 equal-width redshift bins spanning $0.7 \leq z \leq 2$.

1 INTRODUCTION

The issue of constraining the cosmological parameters by employing the 3D galaxy power spectrum as a summary statistic of the matter density perturbations has been widely explored in the last few years. Indeed, the power spectrum estimated from a redshift survey can give a wealth of information through its shape, amplitude and radial anisotropy induced by peculiar velocity-driven redshift space distortions (RSD). In principle the shape can be used to constrain background quantities such as the dark energy equation of state and the geometry of the system that are related to the expansion history of the universe. The amplitude and RSD of galaxy clustering can constrain the growth of cosmological perturbations and the biasing relation between galaxies and mass, i.e. the relation between the spatial distribution of galaxy and the underlying mass density field.

Constraining the growth is essential in order to discriminate dark energy models with the same background properties but different physical origins. This makes the power spectrum a powerful tool in discriminating standard dark energy models from modified gravity theories. However, sharp discrimination is possible only if galaxy bias can be estimated precisely or, at the very least, marginalized over efficiently.

Even though the work of Kaiser (1987) made it clear that one of the most promising ways to determine the fluctuation growth is to exploit the redshift distortion effect (see Hamilton (1997) for a review), in the first pioneering works (Seo & Eisenstein, 2003, 2007) dealing with Fisher matrix formalism as a tool to constrain cosmological parameters with redshift surveys, the redshift distortions were in fact considered a sort of “noise” disturbing the measure of the baryon acoustic oscillations peaks. The attitude was to marginalize over the RSD and the growth. Later on, it

was realized that information contained in the redshift distortions could tighten constraints over cosmological parameters (Amendola et al., 2005; Wang, 2008; Linder & Cahn, 2007) and RSD began to be considered as a standard, additional probe (Guzzo et al., 2008), able to constrain both the growth rate and the dark energy responsible for the accelerated expansion of the universe. The growth factor itself began to be regarded as useful information to be exploited rather than to be marginalized over (Amendola et al., 2005; Wang et al., 2010).

However, as noticed in several works (Wang, 2008; Percival & White, 2009; Song & Percival, 2009), the degeneracies between the growth factor $G(z)$, the (linear) bias $b(z)$ and the power spectrum normalization $\sigma_{8,0} \equiv \sigma_8(z=0)$ do not allow us to constrain all three quantities simultaneously. One can only measure combinations such as $f(z)\sigma_8(z) = f(z)G(z)\sigma_{8,0}$, $b(z)\sigma_8(z) = b(z)G(z)\sigma_{8,0}$ or $\beta(z) \equiv f(z)/b(z)$ (e.g. Ross et al. (2006); Guzzo et al. (2008); Blake et al. (2011)), where $f(z)$ is the growth rate, related to the growth factor via $f(z) = d \ln G(z) / d \ln a$ and $a = (1+z)^{-1}$ is the scale factor. The growth rate was originally parametrized by Peebles (1980) as $f(z) = \Omega_m(z)^{0.6}$ in a matter-dominated cosmology. This expression was later generalized as $f(z) = \Omega_m(z)^\gamma$ to accurately describe the growth rate in a variety of cosmological models ranging from Dark Energy models to non-standard gravity theories (Lahav et al., 1991; Wang & Steinhardt, 1998; Amendola & Quercellini, 2004; Linder, 2005; Polarski & Gannouji, 2008). This parametrization obviously implies $G(z) = \int \Omega_m^\gamma / (1+z) dz$.

Several authors have adopted different strategies to break, bypass or ignore the degeneracy between $G(z)$, $b(z)$ and $\sigma_{8,0}$ depending on the parameters they were interested in constraining.

- In general one fixes (or assumes external priors for) one

of the parameters and then estimate the others. Different authors have fixed the clustering amplitude $\sigma_{8,0}$ to the value estimated from the cosmic microwave background (CMB) data to constrain $f(z)$ and $b(z)$ (e.g. Di Porto et al. 2012) or the growth parameter γ (e.g. Di Porto et al. 2012; Belloso et al. 2011) or both the bias and the growth (e.g. Di Porto et al. 2012). Instead of fixing $\sigma_{8,0}$ to a single value, some authors have assumed CMB priors for this parameter to constrain $f(z)$ (e.g. Guzzo et al. 2008) or γ and $b(z)$ (Gaztanaga et al., 2011).

- One can assume that General relativity holds and fix γ to the Λ cold dark matter (Λ CDM) value (e.g. Seo & Eisenstein 2003; Amendola et al. 2005; Ross et al. 2006; Wang et al. 2010). For example Hawkins et al. (2003) and Cole et al. (2005) fix γ to estimate the bias while Percival et al. (2004) assume a further prior on Ω_m to determine $\sigma_{8,0}$.

- Alternatively, one can consider some measurable combination of the above parameters that can also discriminate models efficiently. A popular choice is the “mass weighted” growth rate $f(z)\sigma_8(z)$ which provides a good test for dark energy models (e.g. Song & Percival 2009; White et al. 2009; Percival & White 2009; Blake et al. 2011; Carbone et al. 2011; Wang et al. 2010)

It is a fact that galaxy bias, growth and clustering amplitude cannot be independently estimated from the observed $P(k)$ alone (Percival & White, 2009) and yet effective constraints can be placed provided that these quantities could be accurately parametrized under fairly general hypotheses. Although the idea is somewhat implicit in some of the works quoted above, it seems to us it has not been clearly pointed out nor discussed thoroughly anywhere. The scope of this work is to make it explicit with a simple proof, that we present in Sec. 2. In Sec. 3 we present the Fisher matrix method that we employ in order to obtain the aforementioned constraints on parameters. Results are presented in Sec. 4 and finally in Sec. 5 we draw our conclusions.

2 LIFTING PARAMETER DEGENERACY

Let us consider a measurement of the galaxy power spectrum in redshift space at different epochs, i.e. in different redshift bins z . In the linear regime, the shape of the power spectrum and its redshift distortions can be modeled as follows (Seo & Eisenstein, 2003, 2007)

$$P_{\text{obs}}(z; k, \mu) = \frac{D_F^2(z)H(z)}{D^2(z)H_F(z)} G^2(z) b^2(z) \sigma_{8,0}^2 \left[1 + \frac{f(z)}{b(z)} \mu^2 \right]^2 P_0 + P_s(z) \\ \equiv C(z) G^2(z) B^2(z) [1 + R(z) \mu^2]^2 P_0 + P_s(z) \quad (1)$$

where $B(z) \equiv b(z)\sigma_{8,0}$, $R(z) = \frac{f(z)\sigma_{8,0}}{B(z)}$, μ is the direction cosine and $P_0 \equiv P(k, z = 0)$ is the linear power spectrum at the present epoch. The factor $C(z) \equiv D_F^2(z)H(z)/(D^2(z)H_F(z))$, where $D(z)$ is the angular diameter distance and $H(z)$ is the Hubble parameter, takes into account the difference in comoving volume between the fiducial cosmology - the one we use to convert observed redshifts into distances - (subscript F) and the true cosmology. Finally, we model the shot noise contribution as an additional factor $P_s(z)$.

However, let us notice that, since we are not interested in constraining $D(z)$ and $H(z)$ in every redshift bin, but only the parameters they depend on, these functions and their combination $C(z)$ are not considered further in this Letter.

Let us assume that the growth rate can be modelled as $\Omega_m(z)^\gamma$. The growth index γ needs not to be constant. The simple parametrization $\gamma(z) = \gamma_0 + \gamma_1 z/(1+z)$ has been shown to reproduce the time dependence of γ in a variety of non standard gravity models (Fu et al., 2009). For the sake of simplicity we consider in this Section the case of constant γ , but our conclusion remains valid also with time-dependent growth index, as we argue below.

Cosmological parameters are determined by fitting Eq. (1) to the observed galaxy power spectrum. From the spectral shape in the linear regime, P_0 , one can determine those parameters that describe the expansion history $H(z)$ (and then $D(z)$) (h , $\Omega_{m,0}$, Ω_{DE} , w_0 , w_1 , etc...). From the amplitude of the power spectrum one determines the combination $A(z) \equiv G(z)B(z)$. If this analysis can be performed at two (or more) redshifts and the growth rate is modelled as $f = \Omega_m(z)^\gamma$, then the degeneracy can be broken. Let us prove it for the simple case in which the power spectrum has been measured at two redshifts z_1 and z_2 . In this case, one determines A and R at two different epochs, A_1 , R_1 , A_2 , R_2 and can solve the linear system

$$A_1 = G_1(\gamma)B_1 \quad (2)$$

$$A_2 = G_2(\gamma)B_2 \quad (3)$$

$$R_1 = \frac{\Omega_{m,1}^\gamma \sigma_{8,0}}{B_1} = \frac{\Omega_{m,1}^\gamma \sigma_{8,0} G_1(\gamma)}{A_1} \quad (4)$$

$$R_2 = \frac{\Omega_{m,2}^\gamma \sigma_{8,0}}{B_2} = \frac{\Omega_{m,2}^\gamma \sigma_{8,0} G_2(\gamma)}{A_2} \quad (5)$$

By assumption Ω_{m,z_i} has been already determined because it depends only on the background parameters. Then the ratio of the last two equations yields

$$\frac{R_1 A_1}{R_2 A_2} = \left(\frac{\Omega_{m,1}}{\Omega_{m,2}} \right)^\gamma \frac{G_1(\gamma)}{G_2(\gamma)} \quad (6)$$

where the only unknown is γ and therefore we can solve for it. Then, from the above equations, one estimates $\sigma_{8,0}$ and $b(z)$ as

$$\sigma_{8,0} = \frac{A_i R_i}{G_i(\gamma) \Omega_{m,i}^\gamma} \quad \text{and} \quad b(z_i) = \frac{\Omega_{m,i}^\gamma}{R_i} \quad (7)$$

We notice that if the power spectrum is measured in three redshift bins, then one can also constrain the time dependence of the growth index $\gamma(z) = \gamma_0 + \gamma_1 z/(1+z)$. This procedure assumes that the size of the bins and the number densities of galaxies within are large enough to provide effective constraints to avoid that parameters’ degeneracy, although broken in principle, can reappear due to poor statistics. As we show in the next section, this is, however, not of concern for large surveys as Euclid. The proof that the degeneracy can be broken can be also obtained using the Fisher matrix formalism (Fisher, 1935; Tegmark et al., 1997). If one assumes $f = \Omega_m(z)^\gamma$, a constant growth index and the model power spectrum of Eq. (1), then the deriva-

tives of the spectrum with respect to $b(z)$, γ and $\sigma_{8,0}$

$$\frac{\partial \ln P_{\text{obs}}}{\partial \ln b_{z_i}} = 2 - 2 \frac{\Omega_m(z_i)^\gamma \mu^2}{b_{z_i} + \Omega_m(z_i)^\gamma \mu^2} \quad (8)$$

$$\frac{\partial \ln P_{\text{obs}}}{\partial \gamma} = 2 \frac{\partial \ln G}{\partial \gamma} + 2 \frac{\Omega_m(z_i)^\gamma \ln \Omega_m(z_i) \mu^2}{b_{z_i} + \Omega_m(z_i)^\gamma \mu^2} \quad (9)$$

$$\frac{\partial \ln P_{\text{obs}}}{\partial \sigma_{8,0}} = \frac{2}{\sigma_{8,0}} \quad (10)$$

are not degenerate because of their different dependence from z and μ . Dropping the γ parametrization, i.e. treating $G(z)$ as an extra free parameter for every bin, would not allow us to lift the parameter degeneracy and a singular Fisher matrix would result. We note that here we assumed the bias to be scale-independent which should be true on the large, linear scales we are focusing on here. A possible scale dependence would modify the shape of the spectrum and should be accounted for to avoid systematic errors in the estimate of the background cosmology parameters. Furthermore, a scale-dependent bias could make the Fisher matrix degenerate again and cause the parameter degeneracies to return. Clearly, in order to break the degeneracy in presence of a bias scale dependence, one should parametrize it as, e.g., a simple power law of k , employing a number of parameters smaller than the number of distinct redshift bins. This issue will be studied in a future work.

3 FISHER MATRIX FORECASTS

We now apply the strategy outlined above to a specific measurement and adopt the Fisher matrix approach to evaluate the expected errors on the measured parameters. For this purpose we choose a reference cosmological model and run CAMB (Lewis et al., 2000) to obtain the linear power spectrum in real space P_0 .

Then, the model power spectrum in Eq. 1 depends on a number of cosmological parameters, listed in Tab. 1. In the upper part we list parameters that do not depend on redshift. Redshift-dependent parameters are listed in the bottom part of the table. In our application we consider the more general case of a time-dependent growth index $\gamma(z) = \gamma_0 + \gamma_1 z / (1 + z)$. We adopt a slightly unconventional fiducial Λ CDM model with $\gamma_0 = 0.545$, and $\gamma_1 = 0$ (to be compared with the concordance Λ CDM values $\gamma_0 = 0.556$, $\gamma_1 = -0.018$ (Fu et al., 2009)) and allow for a time-dependent equation of state for the Dark Energy with $w_0 = -0.95$ and $w_1 = 0$.

In this work we do not consider a possible smearing of the wiggles associated with baryonic acoustic oscillation (BAO) (Seo & Eisenstein, 2007). Further, we ignore non-linear effects that modify the spectral shape and the RSD pattern on small scales (e.g. Blake et al. (2011)) by limiting our analysis to small wavenumbers $k \leq k_{\text{max}} \equiv \min[k_{\text{cut}}, k_{\text{lin}}(z)]$, where k_{cut} is set to $0.2 h \text{Mpc}^{-1}$. The value for $k_{\text{lin}}(z)$ is set by requiring that the variance in cells $\sigma^2(k_{\text{lin}}, z) = 0.25$ (for example, at $z = 0.7$ we have $k_{\text{lin}} \sim 0.16 h \text{Mpc}^{-1}$).

Having assumed our model power spectrum and set the parameter values of the fiducial model, we compute the elements of the Fisher matrix as in Tegmark (1997) by integrating over all modes below k_{max} . The result depends on the

Table 1. List of the parameters that characterize the background cosmology and the model power spectrum. They are used in the Fisher matrix analysis. Redshift dependent parameters are listed in the lower part of the table.

Redshift-independent parameters		fiducial values
Reduced total matter density	$\Omega_{m,0} h^2$	$0.271 \cdot (0.703)^2$
Reduced baryon density	$\Omega_{b,0} h^2$	$0.045 \cdot (0.703)^2$
Curvature density	Ω_k	0
Hubble constant at present	h	0.703
Primordial fluctuation slope	n_s	0.966
Dark energy eq. of state	w_0, w_1	-0.95, 0
Power spectrum normalization	$\sigma_{8,0}$	0.809
γ -parameterization parameters	γ_0, γ_1	0.545, 0
Redshift-dependent parameters (in 14 z -bins)		
Shot noise	P_s	0
Bias	$\log b$	Derived from Orsi et al. (2010)

characteristics of the galaxy redshift catalogue used to compute the power spectrum. More precisely, it depends on the volume of the survey and on the galaxy redshift distribution dN/dz . In this work we take, as a reference case, the Euclid redshift survey as specified in the *Red Book* (Editorial Team et al., 2011) and at the website <http://www.euclid-ec.org/>. This survey will span a broad redshift range $0.7 \leq z \leq 2$ that we split in 14 bins of $\Delta z = 0.1$. The expected sky coverage is 15000 deg^2 . The expected dN/dz is given in the aforementioned *Red Book*, while the fiducial values for the bias in each redshift bin, for Euclid galaxies, are derived from Orsi et al. (2010).

4 RESULTS

Our analysis allows us to set simultaneous constraints on $b(z)$, σ_8 and γ , when the power spectrum is measured at two or more redshifts. Tabs. 2,3 display the expected 1σ uncertainties on these (and other) parameters, listed in the first row. Errors on each parameter are obtained after marginalizing over all other parameters in the table. Therefore they do not coincide with the length of the ellipses' axis shown in Fig. 1 which represent joint, rather than marginalized, probabilities. Table 2 shows the uncertainties on the redshift independent parameters listed in the top row. In the second row the values refer to 1σ uncertainties computed marginalizing over all other parameters while in the bottom row they are obtained through marginalization after fixing γ_1 in order to compare our results to other, similar analysis. In Table 3 we list the expected uncertainties on the bias parameter estimated at the different redshifts specified in the top row. The meaning of the second and third rows is the same as in Table 2.

In the case of a time-dependent growth index, uncertainties on the parameters are remarkably small $\Delta\sigma_8 = 0.03$, $\Delta\gamma_0 = 0.19$ and $b(z) = 2 - 4\%$ depending on the redshift. They decrease even further if γ is assumed to be constant ($\Delta\sigma_8 = 0.007$, $\Delta\gamma = 0.03$ and $\Delta b(z) = 1 - 1.7\%$). In Fig. (1) we plot the confidence regions of γ_0 and σ_8 . Contours refer to 68% and 95% joint probability levels. The blue,

dotted ellipses refer to the case in which we marginalize over all parameters, including $b(z)$. The contour levels shrink considerably when one fixes the value of γ_1 (red, dashed) and become tiny in the case in which all cosmological parameters and the bias are fixed to their fiducial values (we leave only the shot noise free to vary). This last case represents the ideal situation in which the available complementary probes (e.g. SN Ia, CMB fluctuations, lensing etc) allow us to estimate all other parameters with very high precision.

In Fig. 2 we show the analogous confidence contour levels in the $\sigma_8 - b(z)$ (left-hand panel) and $\gamma - b(z)$ (right-hand panel) planes. As in the left-hand panel of Fig. 1 ellipses of different sizes refer to marginalization over different sets of parameters. The four sets of ellipses refer to different redshift slices, as specified by the labels. We do not show all 14 redshifts to avoid overcrowding. Keeping γ constant and assuming a flat universe allows to reduce errors on σ_8 significantly but has little effect on galaxy bias uncertainties.

Finally, we have tested the sensitivity of our result to k_{cut} , i.e. to the cut we have imposed to exclude nonlinear effects. Increasing k_{cut} increases the number of k -modes used in the analysis and reduces statistical errors. However, if k_{cut} is too large, non-linear effects kick in and induce systematic errors. Decreasing k_{cut} allows to apply linear theory but increases random errors. To find the best tradeoff one needs to estimate the power spectrum in some simulated galaxy catalog obtained from fully nonlinear N-body simulations. However, we can obtain an order of magnitude estimate for the relative importance of non-linear effects by re-computing errors at different values of k_{cut} and check how much they change.

The right-hand panel of Fig. 1 shows the result of such exercise in the $\gamma_0 - \sigma_8$ plane. Ellipses filled with different shades of blue represent the reference case of $k_{\text{cut}} = 0.2 h \text{ Mpc}^{-1}$ (and correspond to the blue, short-dashed ellipses in the left panel). Pushing k_{cut} up to $0.5 h \text{ Mpc}^{-1}$ (red, long-dashed) has a little effect, meaning that the decrease in statistical errors does not justify the risk of introducing systematic errors driven by nonlinear effects. Reducing k_{cut} to $0.1 h \text{ Mpc}^{-1}$ has a quite dramatic effect (purple, dotted ellipses). The large increase in the errors reflects the fact that with this k_{cut} one cuts off all but one of the BAO wiggles. Finally, a value of $k_{\text{cut}} = 0.15 h \text{ Mpc}^{-1}$ (black, dot-dashed ellipses) seems to represent a safer and yet acceptable option. However, the optimal choice of k_{cut} depends on the underlying cosmological model and on the accurate modeling of nonlinear effects.

5 CONCLUSIONS

The goal of this Letter is to point out explicitly that a two-point statistics like the power spectrum can provide independent constraints on the cosmological parameters $\sigma_{8,0}$, γ and the galaxy bias, under the quite general assumption that the growth rate of density fluctuation can be parametrized as $f = \Omega_m(z)^\gamma$ and the measurement is performed at two (or more) different redshifts. This result is not surprising. In fact it may appear even obvious, but to the best of our knowledge it has never been explicitly pointed out in the literature. To assess how precisely these parameters can be determined after breaking the degeneracy we have performed a

Fisher-Matrix analysis and explored the case of the next generation Euclid redshift survey (Editorial Team et al., 2011). We found that these quantities could be measured to the percent level. Constraints tighten considerably if a flat universe is assumed or if γ is taken to be time independent. We find that σ_8 and γ can be measured to within 1%, 5%, respectively, while the bias $b(z)$ can be measured to within 1 – 2% (assuming flatness) in every redshift bin.

This procedure can be applied to redshift surveys like WiggleZ (Blake et al., 2011) that are deep enough to provide independent redshift shells in which to measure the power spectrum. Analyses of this dataset have provided estimates of combinations $f\sigma_{8,0}G(z)$ and $\beta(z)$ (Blake et al., 2011). We will investigate the possibility of using the WiggleZ to estimate σ_8 , γ and $b(z)$ in a future paper.

6 ACKNOWLEDGMENTS

We thank Will Percival for his comments on a preliminary version of this work and B. Garilli and the NISP simulations group for providing us with the predicted galaxy redshift distribution for Euclid, as presented in the Euclid Red Book, and the Euclid Consortium for allowing access to this information. CDP acknowledges the support provided by INAF through a PRIN/2008/1.06.11.10 grant. CDP also thanks the Institut für Theoretische Physik and the University of Heidelberg for the kind hospitality and Carmelita Carbone for useful discussions on this topic. EB acknowledges the support provided by MIUR PRIN 2008 “Dark energy and cosmology with large galaxy surveys” and by Agenzia Spaziale Italiana (ASI-Uni Bologna-Astronomy Dept. ‘Euclid-NIS’ I/039/10/0). L.A. acknowledges funding from DFG through the project TRR33 “The Dark Universe”.

References

- Amendola L., Quercellini C., 2004, Phys. Rev. Lett., 92, 181102, arXiv:astro-ph/0403019. 1
- Amendola L., Quercellini C., Giallongo E., 2005, MNRAS, 357, 429, arXiv:astro-ph/0404599 [astro-ph]. 1, 2
- Belloso A. B., Garcia-Bellido J., Sapone D., 2011, JCAP, 1110, 010, arXiv:1105.4825 [astro-ph.CO]. 2
- Blake C., Brough S., Colless M., Contreras C., Couch W., et al., 2011, MNRAS, 415, 2876-2891, arXiv:1104.2948 [astro-ph.CO]. 1, 2, 3, 4
- Carbone C., Verde L., Wang Y., Cimatti A., 2011, JCAP, 1103, 030, arXiv:1012.2868 [astro-ph.CO]. 2
- Cole S., et al., 2005, MNRAS, 362, 505, arXiv:astro-ph/0501174. 2
- Di Porto C., Amendola L., Branchini E., 2012, MNRAS, 419, 985, arXiv:1101.2453 [astro-ph.CO] 2
- Editorial Team, Laureijs R., Amiaux J., Arduini S., Augeres J.-L., et al., 2011, arXiv:1110.3193 [astro-ph.CO]. 3, 4
- Fisher R. A., 1935, J. Roy. Stat. Soc., 98, 39. 2
- Fu X.-y., Wu P.-x., Yu H.-w., 2009, Phys.Lett., B677, 12, arXiv:0905.1735 [gr-qc]. 2, 3
- Gaztanaga E., Eriksen M., Crocce M., Castander F., Fos- alba P., et al., 2011, arXiv:1109.4852 [astro-ph.CO]. 2

<i>Par.</i>	h	$\Omega_{m,0}$	$\Omega_{b,0}$	n	Ω_{DE}	w_0	w_1	γ_0	γ_1	$\sigma_{8,0}$
1σ	0.008	0.004	0.0008	0.03	0.009	0.07	0.31	0.19	0.49	0.03
1σ	0.008	0.004	0.0008	0.02	0.009	0.07	0.28	0.03	-	0.007

Table 2. Uncertainties on cosmological parameters, collectively indicated as *Par.* In the second row 1σ values refer to 68% probability regions computed marginalizing over all other parameters while in the third row values are obtained through marginalization after fixing γ_1 .

z	0.7	0.8	0.9	1.0	1.1	1.2	1.3	1.4	1.5	1.6	1.7	1.8	1.9	2.0
1σ	0.023	0.022	0.022	0.023	0.025	0.027	0.029	0.031	0.034	0.038	0.039	0.041	0.044	0.046
1σ	0.010	0.011	0.011	0.012	0.013	0.014	0.016	0.016	0.018	0.02	0.021	0.022	0.024	0.026

Table 3. In this Table we show the 1σ uncertainties over bias parameters in each redshift bin: in the second row 1σ values refer to uncertainties computed marginalizing over all other parameters while in the third row values are obtained through marginalization after fixing γ_1 and Ω_K .

- Guzzo L., Pierleoni M., Meneux B., Branchini E., Fevre O., et al., 2008, *Nature*, 451, 541, arXiv:0802.1944 [astro-ph]. 1, 2
- Hamilton A., 1997, published in *The Evolving Universe*. Edited by D. Hamilton, Kluwer Academic, 1998, p. 185-275, arXiv:astro-ph/9708102 [astro-ph]. 1
- Hawkins E., et al., 2003, *MNRAS*, 346, 78, arXiv:astro-ph/0212375. 2
- Kaiser N., 1987, *MNRAS*, 227, 1 1
- Lahav O., Lilje P. B., Primack J. R., Rees M. J., 1991, *Mon. Not. Roy. Astron. Soc.*, 251, 128 1
- Lewis A., Challinor A., Lasenby A., 2000, *Astrophys.J.*, 538, 473, arXiv:astro-ph/9911177 [astro-ph]. 3
- Linder E. V., 2005, *Phys. Rev.*, D72, 043529, arXiv:astro-ph/0507263. 1
- Linder E. V., Cahn R. N., 2007, *Astropart.Phys.*, 28, 481, arXiv:astro-ph/0701317 [astro-ph]. 1
- Orsi A., Baugh C., Lacey C., Cimatti A., Wang Y., et al., 2010, *MNRAS*, 405, 1006, arXiv:0911.0669 [astro-ph.CO]. 3
- Peebles J., 1980, *The Large-Scale Structure of the Universe*. Princeton University Press 1
- Percival W. J., White M., 2009, *MNRAS*, 393, 297, arXiv:0808.0003. 1, 2
- Percival W. J., et al., 2004, *MNRAS*, 353, 1201, arXiv:astro-ph/0406513 [astro-ph]. 2
- Polarski D., Gannouji R., 2008, *Phys. Lett.*, B660, 439, arXiv:0710.1510 [astro-ph]. 1
- Ross N. P., et al., 2007, *MNRAS*, 381, 573, arXiv:astro-ph/0612400. 1, 2
- Seo H.-J., Eisenstein D. J., 2003, *Astrophys.J.*, 598, 720, arXiv:astro-ph/0307460 [astro-ph]. 1, 2
- Seo H.-J., Eisenstein D. J., 2007, *Astrophys.J.*, 665, 14, arXiv:astro-ph/0701079 [astro-ph]. 1, 2, 3
- Song Y.-S., Percival W. J., 2009, *JCAP*, 0910, 004, arXiv:0807.0810 [astro-ph]. 1, 2
- Tegmark M., 1997, *Phys.Rev.Lett.*, 79, 3806, arXiv:astro-ph/9706198 [astro-ph]. 3
- Tegmark M., Taylor A., Heavens A., 1997, *Astrophys.J.*, 480, 22, arXiv:astro-ph/9603021 [astro-ph]. 2
- Wang L.-M., Steinhardt P. J., 1998, *Astrophys. J.*, 508, 483, arXiv:astro-ph/9804015. 1
- Wang Y., 2008, *JCAP*, 0805, 021, arXiv:0710.3885 [astro-ph]. 1
- Wang Y., Percival W., Cimatti A., Mukherjee P., Guzzo L., et al., 2010, *MNRAS*, 409, 737, arXiv:1006.3517 [astro-ph.CO]. 1, 2
- White M., Song Y.-S., Percival W. J., 2009, *MNRAS*, 397, 1348, arXiv:0810.1518. 2

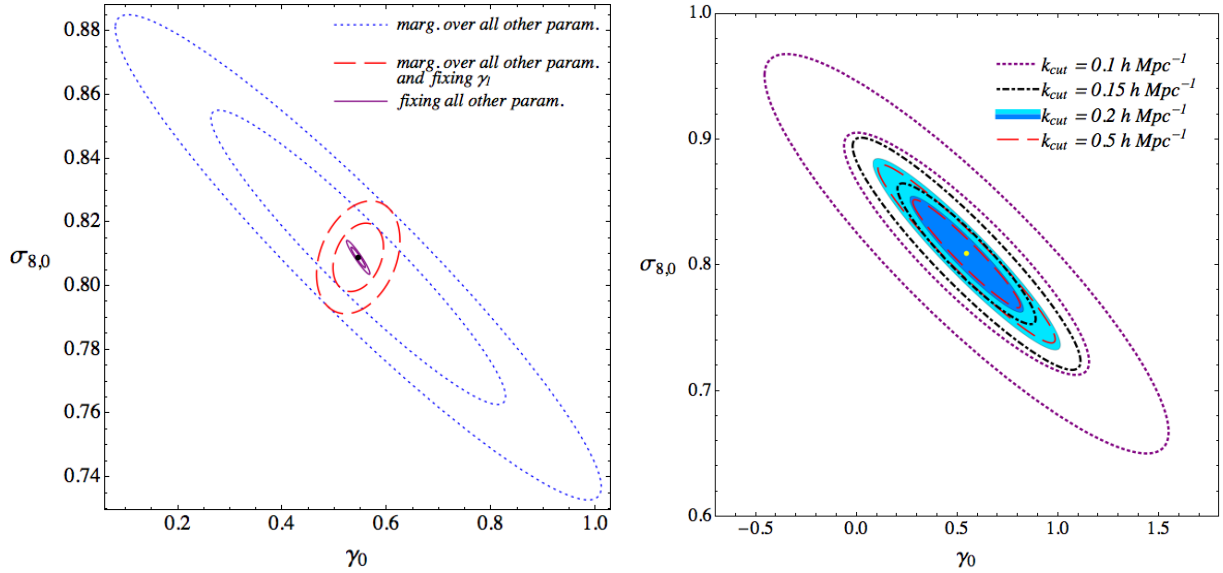


Figure 1. Left-hand panel: contours at 68% and 95% of probability for the parameters γ_0 and $\sigma_{8,0}$ when *i*) we marginalize over all other parameters (blue, dotted ellipses); *ii*) we marginalize over all other parameters after fixing γ_1 (red, long-dashed ellipses) and *iii*) we fix all other parameters. The last case is represented by the very small purple, solid ellipses nearly overlapping on the black dot which marks the fiducial model. The marginalized 1σ errors for $\sigma_{8,0}$ are 0.03, 0.007, 0.002 for the 3 cases, respectively while those for γ are 0.19, 0.03, 0.009. Right-hand panel: contours at 68% and 95% of probability for the parameters γ_0 and $\sigma_{8,0}$ varying k_{cut} .

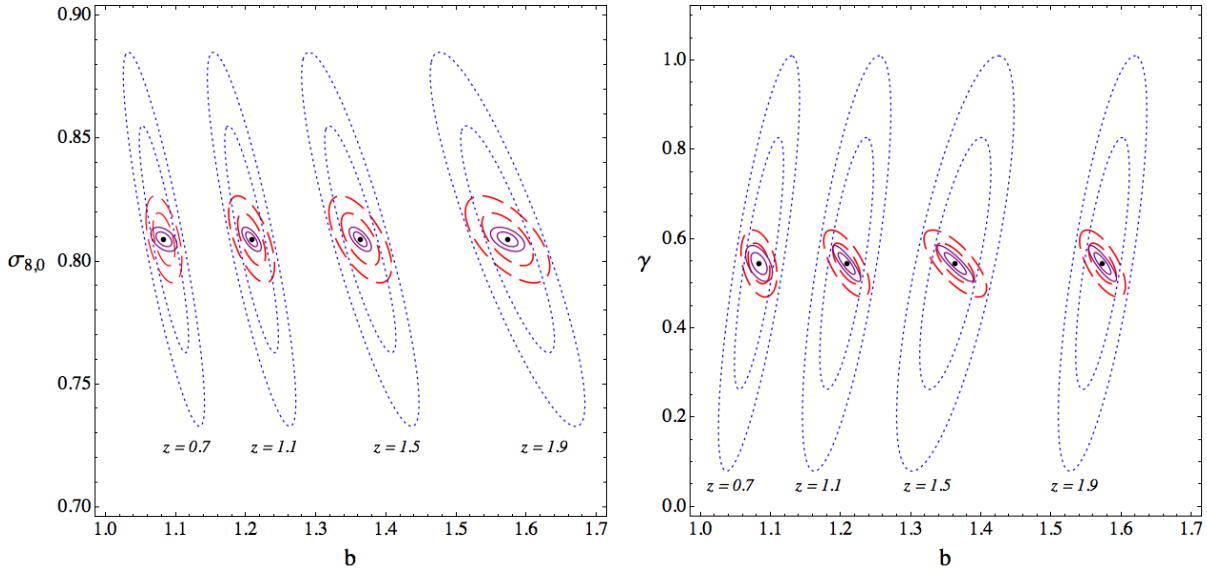


Figure 2. Left-hand panel: the three sets of ellipses show the contours at 68% and 95% of probability for the parameters $\sigma_{8,0}$ and $b(z)$ in 4 redshift bins when *i*) we marginalize over all other parameters (blue, dotted ellipses); *ii*) we marginalize over all other parameters after fixing γ_1 and Ω_K (red, long-dashed ellipse) and *iii*) we fix all other parameters (purple, solid ellipses). The black dots mark the fiducial values for the parameters and are centered at the central values of each redshift bin. Right-hand panel: as in left-hand panel, but for the parameters γ_0 and $b(z)$.